Theor. Comput. Fluid Dyn. (2006) 20: 125–144
DOI 10.1007/s00162-006-0017-y

ORIGINAL ARTICLE

B. J. Binder · F. Dias · J.-M. Vanden-Broeck

Steady free-surface flow past an uneven channel bottom

Received: 26 January 2006 / Accepted: 7 March 2006 / Published online: 9 May 2006

Abstract New free-surface flows past a semi-infinite 'step' in the bottom of a channel are considered. Surface tension is neglected but gravity is included in the dynamic boundary condition. Fully nonlinear solutions are computed by boundary integral equation methods. Additional weakly nonlinear solutions are derived analytically. A thorough analysis of the weakly nonlinear problem provides a systematic approach to identify all the possible types of solutions and the number of independent parameters.

Keywords Free-surface flow, Topography, Boundary integral equation method, Potential flow

PAGS 47.35.-i, 47.15.km, 02.30.Rz, 02.60.Nm

1 Introduction

Free-surface flows past submerged or surface piercing obstacles have many practical applications in hydraulic and coastal engineering, and in ship hydrodynamics. Those include free-surface flows generated by ships and submarines, flows under sluice gates and flows past uneven topographies. The fluid is often assumed to be inviscid and incompressible and the flow to be irrotational. Over the years many fully nonlinear computations have been performed [1,3,5,6,8,9,14]. In addition linear and weakly nonlinear analytical approximations have also been derived [4,7,11,12,16].

Recently Dias and Vanden-Broeck [4] have derived weakly nonlinear approximations for two-dimensional[1] free-surface flows past obstacles with bounded support at the bottom of a horizontal channel. Their approximation is valid when the Froude number is close to criticality (transition from subcritical flow to supercritical flow). Following Lee et al. [10], they showed that the problem can be formulated as a forced Korteweg–de Vries (KdV) equation where each obstacle generates a forcing in the form of a Dirac delta function. Whether the

Communicated by R. Grimshaw

B. J. Binder
School of Mathematical Sciences, University of Adelaide,
Adelaide, Australia

F. Dias (✉)
Centre de Mathématiques et de Leurs Applications,
Ecole Normale Supérieure de Cachan, Cachan, France
E-mail: Frederic.Dias@cmla.ens-cachan.fr

J.-M. Vanden-Broeck
School of Mathematics, University of East Anglia,
Norwich UK

[1] In our terminology, a two-dimensional solution is a solution depending upon only one horizontal space variable, the second dimension being the vertical dimension.

forcing in the KdV equation appears as a delta function depends in fact on scaling; for instance in Grimshaw and Smyth [7] this scaling was kept open and forcings other than delta functions were considered. With a delta function forcing, the flows can then be constructed in a phase plane in which each obstacle appears as a vertical jump (jump in the slope of the free surface). This asymptotic approach provides a systematic way to identify all the possible solutions and the number of parameters necessary to specify them uniquely. In this way Dias and Vanden-Broeck [4] discovered new types of solutions which were subsequently computed in the fully nonlinear regime by boundary integral equation methods.

Binder and Vanden-Broeck [2] used a similar approach to analyse free-surface flows under an inclined sluice gate. They showed that such solutions can also be constructed in a phase plane in which the gate generates a horizontal displacement (change in the elevation of the free surface with constant slope). Previous results were recovered and extended. In particular it was confirmed that there is no steady potential flow which satisfies the radiation condition.

All the obstacles considered by Dias and Vanden-Broeck [3–5] have bounded support. This means that the depth of the channel bottom is the same far upstream and far downstream. In this paper we extend the approach to the case where the depths far upstream and downstream are different. The canonical problem is then the free-surface flow past a step. We show that the phase plane analysis can be extended to this configuration. There are no vertical nor horizontal jumps but instead a superposition of two phase planes. The solutions are then obtained by moving continuously along the orbits from one phase plane to the other. Alternatively, one can consider that there is a jump in the second derivative (curvature) of the free surface [16]. The free-surface flow over a step was studied previously by King and Bloor [8]. While some of our solutions coincide with theirs, some solutions are new. A similar geometry was used by Yasuda et al. [15] to study the interaction between an incoming solitary wave and a reef with a vertical face (submerged breakwater).

A typical flow configuration with a semi-infinite 'step' of height h^* in the bottom of a channel is shown in Fig. 1a. As in all flows considered in this paper, the fluid flows from right to left. The height h^* can be either positive (step up) or negative (step down as shown for example in Fig. 1a). Cartesian coordinates (x^*, y^*) with the origin at the position of the 'step' in the channel bottom are defined.

As $x^* \to \infty$, the flow is assumed to approach a uniform stream with constant velocity $-U$ and constant depth H, see Fig. 1a. We define the upstream Froude number

$$F = \frac{U}{(gH)^{1/2}}, \tag{1}$$

where g is the acceleration due to gravity. The flow as $x^* \to -\infty$ can either approach a uniform stream with constant velocity $-V$ and constant depth $D - h^*$, or possess a train of waves. When the flow is uniform as $x^* \to -\infty$ we define the downstream Froude number

$$F^* = \frac{V}{[g(D - h^*)]^{1/2}}. \tag{2}$$

The following dimensionless numbers are introduced:

$$d = \frac{D}{H}, \quad h = \frac{h^*}{H}. \tag{3}$$

By performing a weakly nonlinear analysis, we will show that there are five basic types of steady solutions: subcritical flows ($F < 1$) with a train of waves downstream, hydraulic falls (subcritical on one side of the step and supercritical on the other side), supercritical flows ($F > 1$ and $F^* > 1$), generalized hydraulic falls ($F > 1$) with a train of waves, and critical flows characterized by $F = 1$. These basic types of solutions are then computed numerically. The details of the formulation and of the numerical scheme are given in the next section. Results are given in Sect. 3.

2 Formulation

The steady two-dimensional irrotational flow of an incompressible inviscid fluid shown in Fig. 1a is considered. It is bounded below by the bottom of the channel $A'B'C'D'$. The equation of the bottom of the channel is denoted by $y^* = \sigma^*(x^*)$. The flow is bounded above by the free surface AB. The equation of the free surface AB can be written as $y^* = H + \eta^*(x^*)$. The function $\eta^*(x^*)$ is assumed to vanish as $x^* \to \infty$.

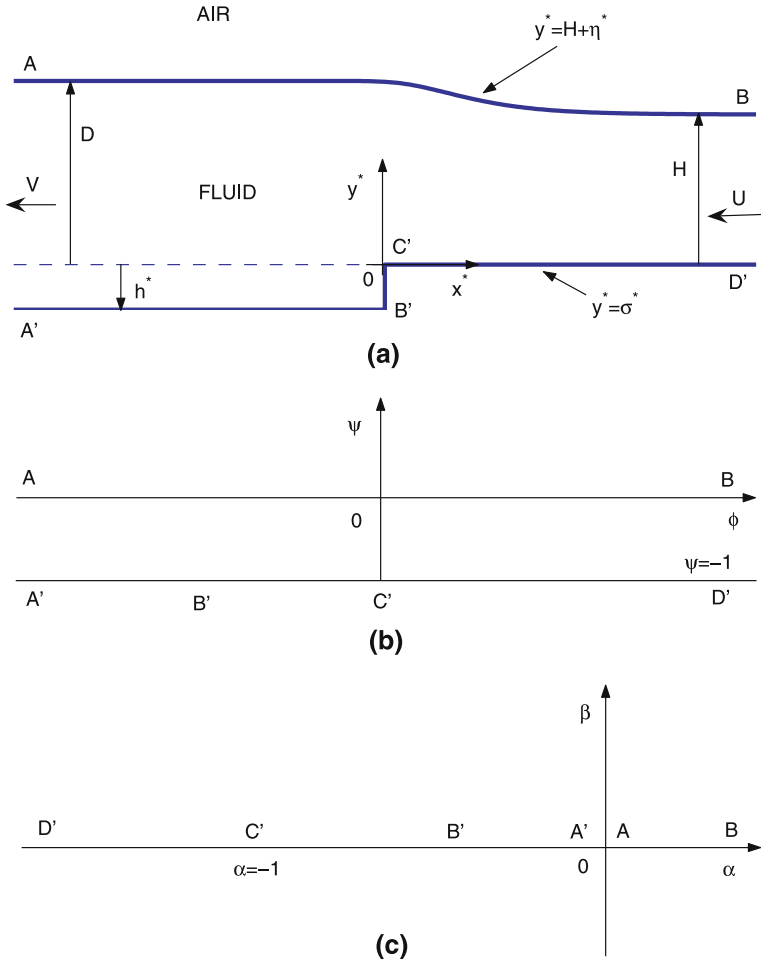

Fig. 1 **a** Sketch of a free-surface flow over a step in physical coordinates (x^*, y^*). **b** Sketch of the flow in the plane of the complex potential (f-plane). **c** Sketch of the flow in the lower half-plane (ζ-plane). Various points have been labelled along the bottom and the free surface

The dynamic boundary condition on the free surface AB gives

$$\frac{1}{2}(u^{*2} + v^{*2}) + gy^* = \frac{1}{2}U^2 + gH \quad \text{on } y^* = H + \eta^*(x^*), \tag{4}$$

where u^* and v^* are the horizontal and vertical components of the velocity. Here, we have used the conditions $u^* \to -U$, $v^* \to 0$, $\eta^*(x^*) \to 0$ as $x^* \to \infty$, in order to evaluate the Bernoulli constant on the right hand side of (4).

As mentioned in Introduction, the flow as $x^* \to -\infty$ can be characterized either by a uniform stream with constant velocity $-V$ and constant depth $D - h^*$ or by a train of waves. When the flow as $x^* \to -\infty$ is uniform, a relation between F, d and h can be derived in the following way. First the conservation of mass implies

$$V(D - h^*) = UH \quad \text{or} \quad (d - h)\frac{V}{U} = 1. \tag{5}$$

Next Eq. (4) evaluated in the limit $x^* \to -\infty$ yields

$$\frac{1}{2}V^2 + gD = \frac{1}{2}U^2 + gH \quad \text{or} \quad \left(\frac{V}{U}\right)^2 + \frac{2d}{F^2} = 1 + \frac{2}{F^2}. \tag{6}$$

Combining (5) and (6) gives the relations

$$\frac{2d}{F^2}(d-h)^2 - \left(1+\frac{2}{F^2}\right)(d-h)^2 + 1 = 0, \tag{7}$$

$$F^* = F\left(\frac{1}{d-h}\right)^{3/2}. \tag{8}$$

Equation (7) provides d (or $d-h$) once h and F are given. Plots of $d-h$ and F^* versus F are shown in Fig. 2 for negative and positive values of h, as well as for $h=0$. For $h>0$, there is a gap in Froude numbers around the critical Froude number $F=1$. At the turning points, it can be shown that

$$h = \frac{1}{2}\left(2+F^2-3F^{2/3}\right), \quad d-h = F^{2/3}, \quad F^* = 1. \tag{9}$$

For $h \neq 0$, there are no solutions with $F = F^*$ $(d-h=1)$. Therefore, there are no solutions for (waveless) supercritical flow with $F = F^* > 1$ nor waveless subcritical flow with $F = F^* < 1$. It is easy to show that solutions with $d=1$ are also impossible. There exists an interesting property of Eq. (7):

$$\text{if } \; h = \frac{1}{2}(F-1)^2, \quad \text{then } d-h = F, \quad d-h = \frac{1}{4}\left(1+\sqrt{1+8F}\right) \tag{10}$$

are exact solutions. The solutions for a step of zero height are interesting to recall because they shed some light on the transition from a step up to a step down. When $h=0$, Eq. (7) reduces to

$$(d-1)\left(\frac{2}{F^2}d^2 - d - 1\right) = 0. \tag{11}$$

Of course, one has the trivial solution $d=1$ with $F=F^*$ but also the nontrivial solution

$$d = \frac{F^2}{4}\left(1+\sqrt{1+\frac{8}{F^2}}\right), \tag{12}$$

sometimes called the Bélanger formula. These solutions have been plotted in Fig. 2c.

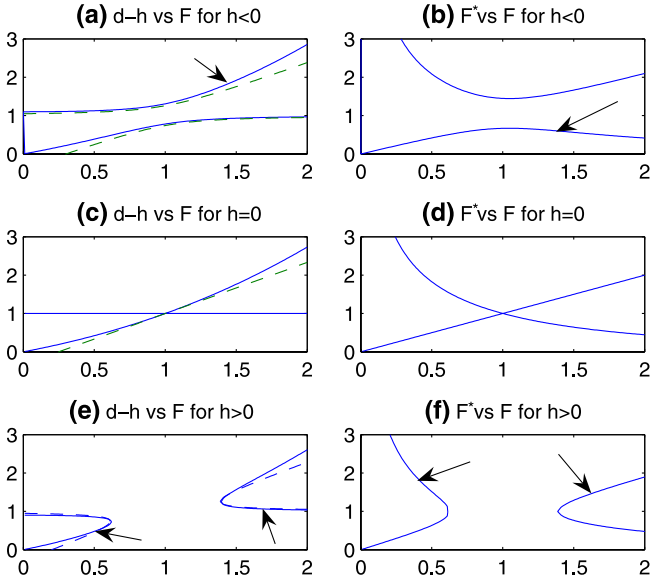

Fig. 2 Exact values of $d-h$ and F^* versus F for $h=-0.1$ (*top*), $h=0$ (*middle*) and $h=0.1$ (*bottom*). The *dashed lines* correspond to the approximate results given by the weakly nonlinear theory. The *arrows* give an indication of the parameter range of the flows computed in the present paper that are uniform as $x^* \to -\infty$

It is also interesting to plot $d - h$ and F^* as a function of h for a given Froude number. This is done in Fig. 3. As shown by King and Bloor [8], it is clear that there is a maximum step size for $h > 0$ (step down),

$$h_{\max} = \frac{1}{2}\left(2 + F^2 - 3F^{2/3}\right) = \frac{1}{2}\left(F^{2/3} - 1\right)^2\left(F^{2/3} + 2\right). \tag{13}$$

As we shall see the determination of the number of independent parameters needed to obtain a unique solution is often delicate and counter intuitive. It can be found by careful numerical experimentation (fixing too many or too few parameters fails to yield convergence). An alternative approach is to perform a weakly nonlinear analysis in the phase space. This second approach has the advantage of allowing a systematic determination of all the possible solutions (within the range of validity of the weakly nonlinear analysis). Both approaches are used in this paper.

The weakly nonlinear analysis will show that one possible type of solution is a (waveless) supercritical flow with $F > 1$ and $F^* > 1$, $F \neq F^*$. If $h > 0$, then $F > F^* > 1$. Such solutions lie along the bottom part of the right branch shown in Fig. 2e and the upper part of the right branch shown in Fig. 2f. They are indicated by an arrow in these two figures. If $h < 0$, then $F^* > F > 1$. Such solutions lie along the right part of the bottom branch shown in Fig. 2a and the right part of the upper branch shown in Fig. 2b.

Another possible type of solution with a uniform stream as $x^* \to \pm\infty$ is a waveless hydraulic fall with $F^* < 1$ and $F > 1$ when $h < 0$ (right part of the upper branch shown in Fig. 2a and right part of the lower branch shown in Fig. 2b) or $F^* > 1$ and $F < 1$ when $h > 0$ (bottom part of the left branch shown in Fig. 2e and upper part of the left branch shown in Fig. 2f). These solutions are indicated by arrows in these figures.

There are in addition three other possible types of solutions, with a train of waves as $x^* \to -\infty$. The first one is a subcritical flow with $F < 1$. The second one is a generalised hydraulic fall with $F > 1$ (see [4] for a detailed description of generalised hydraulic falls). The third one is a critical flow with $F = 1$.

Therefore there are five basic types of solutions considered in this paper. In the next subsection a weakly nonlinear analysis is performed. Then we give details of the formulation of the boundary integral equation method for the fully nonlinear problem.

2.1 Weakly nonlinear theory

Shen [11], Dias and Vanden-Broeck [4], Binder et al. [1] and others derived a forced Korteweg–de Vries equation to model the flow past a disturbance in a channel. Their derivation is based on long wavelength asymptotics. Thus if L denotes a typical horizontal length scale and H is the constant depth as $x^* \to \infty$, we introduce

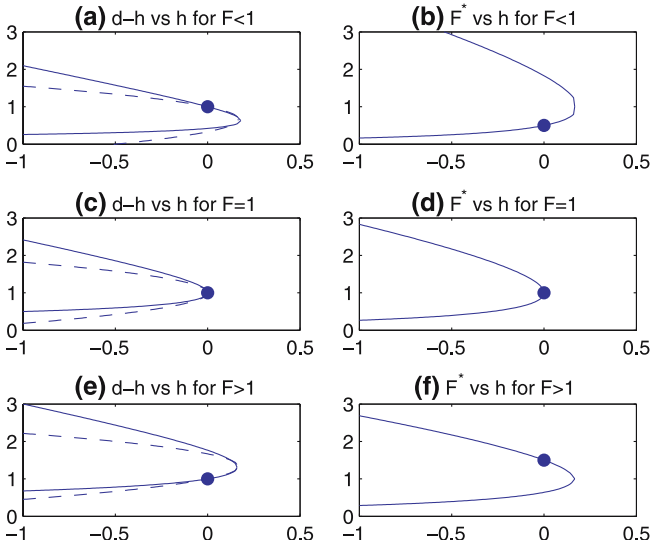

Fig. 3 Exact values of $d - h$ and F^* versus h for $F = 0.5$ (*top*), $F = 1$ (*middle*) and $F = 1.5$ (*bottom*). The *dashed lines* correspond to the approximate results given by the weakly nonlinear theory. The *big dots* correspond to the trivial solution with no step: $h = 0$, $d = 1$

the small parameter $\epsilon = (H/L)^2 \ll 1$, the dimensionless spatial variables $(x', y') = (\epsilon^{1/2}x^*, y^*)/H$ and the free-surface elevation $\epsilon\eta' = \eta^*/H$. The dimensionless equation of the channel bottom is then $y' = \sigma'(x') = \epsilon^{-2}\sigma^*(x^*)/H$. The dimensionless step height is $h = h^*/H$. The Froude number F is written as $F = 1 + \epsilon\mu$.

Substituting expansions in powers of ϵ into the exact potential equations (rewritten in terms of the new scaled variables), the forced KdV equation is derived by equating coefficients of the powers of ϵ. The steady forced KdV equation (rewritten in terms of the variables $x = \epsilon^{-1/2}x'$, $\eta = \epsilon\eta'$ and $\sigma = \epsilon^2\sigma'$ used in the nonlinear computations) is

$$\eta_{xx} + \frac{9}{2}\eta^2 - 6(F-1)\eta = -3\sigma. \tag{14}$$

For $x > 0$, $\sigma = 0$ and Eq. (14) then gives

$$\eta_{xx} + \frac{9}{2}\eta^2 - 6(F-1)\eta = 0. \tag{15}$$

The fixed points ($\eta_x = 0$) are $\eta = 0$ and $\eta = 4/3(F-1)$. For $F > 1$ there is a saddle point at $\eta = 0$, $\eta_x = 0$ and a centre point at $\eta = 4/3(F-1)$, $\eta_x = 0$. For $F < 1$ there is a centre point at $\eta = 0$, $\eta_x = 0$ and a saddle point at $\eta = 4/3(F-1)$, $\eta_x = 0$.

Integrating (15) with respect to x yields

$$\eta_x^2 = 6(F-1)\eta^2 - 3\eta^3 + C. \tag{16}$$

For $F > 1$, a solitary wave orbit is obtained when the constant of integration C is equal to 0. When $C = -32/9(F-1)^3$, the bounded orbit reduces to the centre point. For $F < 1$, the solitary wave orbit is obtained for $C = -32/9(F-1)^3$ and the bounded orbit reduces to the centre point when $C = 0$.

For $x < 0$, $\sigma = h$ and (14) then gives

$$\eta_{xx} + \frac{9}{2}\eta^2 - 6(F-1)\eta = -3h. \tag{17}$$

The situation is slightly more complicated. A discussion on the sign of h is needed.

2.1.1 Step down ($h < 0$)

The fixed points ($\eta_x = 0$) exist for all values of F and are characterized by

$$\eta_1 = \frac{2}{3}(F-1) + \sqrt{\frac{4}{9}(F-1)^2 - \frac{2}{3}h}, \quad \eta_2 = \frac{2}{3}(F-1) - \sqrt{\frac{4}{9}(F-1)^2 - \frac{2}{3}h}. \tag{18}$$

The fixed point labelled with subscript 2 is a saddle point. The fixed point labelled with subscript 1 is a centre. They are nothing else than approximations to the exact values of $d - h - 1$ obtained with Eq. (7). They are represented by the dashed lines in Figs. 2a and 3a, c, e.

Integrating (17) with respect to x yields

$$\eta_x^2 = 6(F-1)\eta^2 - 3\eta^3 - 6h\eta + C_s. \tag{19}$$

For the solitary wave orbit, the value of the constant of integration C_s can be obtained by substituting $\eta_x = 0$ and $\eta = \eta_2$ into (19). The value of C_s at the centre point η_1 can be obtained by substituting $\eta_x = 0$ and $\eta = \eta_1$ into (19).

2.1.2 Step up ($h > 0$)

The fixed points do not exist for all values of F. They are characterized by $\eta_x = 0$ and

$$\eta_1 = \frac{2}{3}(F-1) + \sqrt{\frac{4}{9}(F-1)^2 - \frac{2}{3}h}, \quad \eta_2 = \frac{2}{3}(F-1) - \sqrt{\frac{4}{9}(F-1)^2 - \frac{2}{3}h}. \tag{20}$$

Their existence requires $(F-1)^2 > 3h/2$. The fixed point labelled with subscript 2 is a saddle point. The fixed point labelled with subscript 1 is a centre. They are represented by the dashed lines in Figs. 2e and 3a, e. In (10), it was stated that if $h = (F-1)^2/2$, then $d - h = F$ is an exact solution. It also holds in the framework of the weakly nonlinear analysis: for $h = (F-1)^2/2$, $\eta_2 = F - 1$ if $F < 1$ and $\eta_1 = F - 1$ if $F > 1$.

2.2 Boundary integral equation method

We define dimensionless variables by taking H as the reference length and U as the reference velocity. Thus we define the dimensionless variables $(x, y) = (x^*, y^*)/H$. The equation for the bottom of the channel, A′B′C′D′, is then $y = \sigma(x)$, where $\sigma = \sigma^*/H$. The dimensionless step height is $h = h^*/H$. The free surface AB is then described by $y = 1 + \eta(x)$, where $\eta = \eta^*/H$. The dimensionless horizontal and vertical components of the velocity are u and v respectively.

The dynamic boundary condition (4) is now rewritten as

$$\frac{1}{2}(u^2 + v^2) + \frac{1}{F^2}y = \frac{1}{2} + \frac{1}{F^2}, \tag{21}$$

where F is the Froude number defined by (1). The relation (8) between the upstream and downstream Froude numbers is rewritten as

$$F^* = \frac{F}{[y(-\infty) - h]^{3/2}}. \tag{22}$$

The nonlinear problem can be reduced to a problem in complex analysis (see for example King and Bloor [8]). Since from a mathematical point of view the computed flows are reversible, the direction of the flow does not matter for the computations. This subsection and the next one have been written assuming that the flow goes from left to right. We first introduce the velocity potential ϕ and the stream function ψ. Then the complex potential, $f = \phi + \mathrm{i}\psi$, and the complex velocity, $w = \mathrm{d}f/\mathrm{d}z = u - \mathrm{i}v$ are defined. Without loss of generality we choose $\psi = 0$ on the free-surface streamline AB. On the bottom of the channel we choose $\phi = 0$ at the point C′, which is also the origin of the coordinate system. The value of ϕ at the point B′ is denoted by ϕ_b. It follows from the conservation of mass that $\psi = -1$ on the bottom of the channel A′B′C′D′. The fluid domain in the complex f-plane is the strip $-1 < \psi < 0$, see Fig. 1b.

The strip $-1 < \psi < 0$ is mapped onto the lower half ζ-plane by the transformation

$$\zeta = \alpha + \mathrm{i}\beta = \mathrm{e}^{\pi f}. \tag{23}$$

The flow configuration in the ζ-plane is shown in Fig. 1c.

We define the function $\tau - \mathrm{i}\theta$ by

$$u - iv = e^{\tau - i\theta} \tag{24}$$

and we apply Cauchy's integral formula to the function $\tau - \mathrm{i}\theta$ in the ζ-plane with a contour consisting of the α-axis and a semicircle of arbitrary large radius in the lower half plane. Since $\tau - \mathrm{i}\theta \to 0$ as $|\zeta| \to \infty$, there is no contribution from the half circle and we obtain (after taking the real part)

$$\tilde{\tau}(\alpha) = \frac{1}{\pi}\int_{-\infty}^{\infty} \frac{\tilde{\theta}(\alpha_0)}{\alpha_0 - \alpha}\mathrm{d}\alpha_0, \tag{25}$$

where $\tilde{\tau}(\alpha)$ and $\tilde{\theta}(\alpha)$ are the values of τ and θ on the α-axis. The integral in (25) is to be interpreted in the Cauchy principal value sense.

For a vertical fall in the height h of the horizontal bottom of the channel, the kinematic boundary conditions imply

$$\tilde{\theta}(\alpha) = \pi/2 \quad \text{for } -1 < \alpha < \alpha_\mathrm{b} \tag{26}$$

and

$$\tilde{\theta}(\alpha) = 0 \quad \text{for } \alpha < -1 \text{ and } \alpha_\mathrm{b} < \alpha < 0. \tag{27}$$

Here $\alpha_\mathrm{b} = -\mathrm{e}^{\pi\phi_\mathrm{b}}$. Substituting (26) and (27) in (25) gives

$$\tilde{\tau}(\alpha) = \frac{1}{2}\ln\frac{|\alpha_\mathrm{b} - \alpha|}{|1 + \alpha|} + \frac{1}{\pi}\int_{0}^{\infty} \frac{\theta(\alpha_0)}{\alpha_0 - \alpha}\mathrm{d}\alpha_0. \tag{28}$$

Note that for a vertical rise in the height h of the horizontal bottom of the channel, there is a change in sign in front of the logarithmic term in (28).

We assume that $\alpha > 0$ (i.e. that α corresponds to points on the free surface) and rewrite (28) in terms of ϕ by using the change of variables

$$\alpha = \mathrm{e}^{\pi\phi}, \quad \alpha_0 = \mathrm{e}^{\pi\phi_0}. \tag{29}$$

This gives

$$\tau(\phi) = \frac{1}{2}\ln\frac{\mathrm{e}^{\pi\phi_\mathrm{b}} + \mathrm{e}^{\pi\phi}}{1 + \mathrm{e}^{\pi\phi}} + \int_{-\infty}^{\infty} \frac{\theta(\phi_0)\mathrm{e}^{\pi\phi_0}}{\mathrm{e}^{\pi\phi_0} - \mathrm{e}^{\pi\phi}}\mathrm{d}\phi_0. \tag{30}$$

Here $\tau(\phi) = \tilde{\tau}(\mathrm{e}^{\pi\phi})$ and $\theta(\phi) = \tilde{\theta}(\mathrm{e}^{\pi\phi})$.

Integrating the identity

$$x_\phi + \mathrm{i}y_\phi = \frac{1}{u - \mathrm{i}v} = \mathrm{e}^{-\tau + \mathrm{i}\theta} \tag{31}$$

and equating real and imaginary parts we can obtain parametric relations for the shape of the free surface AB:

$$x(\phi) = x(\infty) + \int_{\infty}^{\phi} \mathrm{e}^{-\tau(\phi_0)}\cos\theta(\phi_0)\mathrm{d}\phi_0 \quad \text{for } -\infty < \phi < \infty \tag{32}$$

and

$$y(\phi) = 1 + \int_{\infty}^{\phi} \mathrm{e}^{-\tau(\phi_0)}\sin\theta(\phi_0)\mathrm{d}\phi_0 \quad \text{for } -\infty < \phi < \infty. \tag{33}$$

Another equation valid on the free surface is obtained by substituting (24) into (21). This yields

$$\mathrm{e}^{2\tau} + \frac{2}{F^2}y = 1 + \frac{2}{F^2}. \tag{34}$$

Equations (30), (33) and (34) define a nonlinear integral equation for the unknown function $\theta(\phi)$ on the free surface $-\infty < \phi < \infty$. We note that the values of $x(\phi)$ and $x(\infty)$ in (32) are not needed to calculate $\theta(\phi)$. Therefore they can be evaluated after a converged solution has been obtained.

2.3 Numerical scheme

The integral equation defined by (30), (33) and (34) is solved numerically. The numerical procedure is similar to the procedure used for example by King and Bloor [8] and later in [1,2,14]. We first introduce the equally spaced mesh points in the potential function ϕ

$$\phi_I = [-(N-1)/2 + (I-1)]\,\Delta, \quad I = 1, \ldots, N. \tag{35}$$

Here $\Delta > 0$ is the mesh size. The corresponding unknowns are

$$\theta_I = \theta(\phi_I), \quad I = 1, \ldots, N. \tag{36}$$

The function τ is evaluated at the midpoints

$$\phi_{I+1/2} = \frac{\phi_I + \phi_{I+1}}{2}, \quad I = 1, \ldots, N-1, \tag{37}$$

by applying the trapezoidal rule to the integral in (30) with summation over the points ϕ_I. The symmetry of the quadrature and of the distribution of the points enables us to evaluate the Cauchy principal value as if it were an ordinary integral.

The dynamic boundary condition (34) can be satisfied at the midpoints (37), using (33). This yields $N-1$ nonlinear algebraic equations. In the remaining of the paper we shall refer to this system of $N-1$ equations as the system [A].

The values of θ are known on the bottom of the channel defined by $\psi=-1$. In order to calculate the size of the step, we need to evaluate τ on $\psi=-1$. This is done by replacing the change of variables (29) by

$$\alpha=-\mathrm{e}^{\pi\phi},\quad \alpha_0=\mathrm{e}^{\pi\phi_0}. \tag{38}$$

Proceeding as in the derivation of (30), we obtain

$$\tau^{\mathrm{B}}(\phi)=\frac{1}{2}\ln\frac{|-\mathrm{e}^{\pi\phi_{\mathrm{b}}}+\mathrm{e}^{\pi\phi}|}{|-1+\mathrm{e}^{\pi\phi}|}+\int_{-\infty}^{\infty}\frac{\theta(\phi_0)\mathrm{e}^{\pi\phi_0}}{\mathrm{e}^{\pi\phi_0}+\mathrm{e}^{\pi\phi}}\mathrm{d}\phi_0. \tag{39}$$

The step height, h, can then be obtained by integrating (31)

$$y^{\mathrm{B}}(\phi)=\int_{0}^{\phi}\mathrm{e}^{-\tau^{\mathrm{B}}(\phi_0)}\mathrm{d}\phi_0\quad\text{for }\phi_{\mathrm{b}}<\phi<0. \tag{40}$$

We define equally spaced mesh points by

$$\phi_I^{\mathrm{B}}=(I-1)\frac{\phi_{\mathrm{b}}}{(N^{\mathrm{B}}-1)},\quad I=1,\ldots,N^{\mathrm{B}}, \tag{41}$$

and τ^{B} is evaluated at the midpoints

$$\phi_{I+1/2}^{\mathrm{B}}=\frac{\phi_I^{\mathrm{B}}+\phi_{I+1}^{\mathrm{B}}}{2},\quad I=1,\ldots,N^{\mathrm{B}}-1, \tag{42}$$

by integrating (39) numerically. Substituting these values of τ^{B} into (40) and integrating numerically we obtain $y^{\mathrm{B}}(\phi)$. The step height is then given by

$$h=y^{\mathrm{B}}(\phi_{\mathrm{b}}). \tag{43}$$

The system of nonlinear algebraic equations obtained after discretization is solved by Newton's method. Fully nonlinear free-surface profiles and fully nonlinear phase trajectories are discussed and presented in Sect. 3.

In the next section we present new weakly nonlinear and fully nonlinear free-surface profiles for the flow past a step in the bottom of a channel. The range of validity of the weakly nonlinear theory is determined by comparing weakly nonlinear and fully nonlinear profiles.

3 Results

In most of the figures providing numerical results (see for example Fig. 4), four plots are given: (a) fully nonlinear free-surface profile $y=1+\eta(x)$, (b) fully nonlinear phase plane (η,η_x), (c) weakly nonlinear free-surface profile, (d) weakly nonlinear phase plane (η,η_x). In (d), the dashed (resp. solid) curves represent various orbits for $x>0$ (resp. $x<0$). These orbits are the same for all configurations. They correspond to orbits of the KdV equation: there is a solitary wave (homoclinic orbit) leaving the saddle point, going beyond the centre and coming back to the saddle point, and there are cnoidal waves (periodic orbits) going around the centre. The bold curve indicates the computed solution, obtained as the intersection between a dashed orbit (flow upstream of the step, $x>0$, $h=0$) and a solid orbit (flow downstream of the step, $x<0$, $h\neq 0$). The arrows along the bold curve indicate the trajectory as one goes from left to right along the free surface.

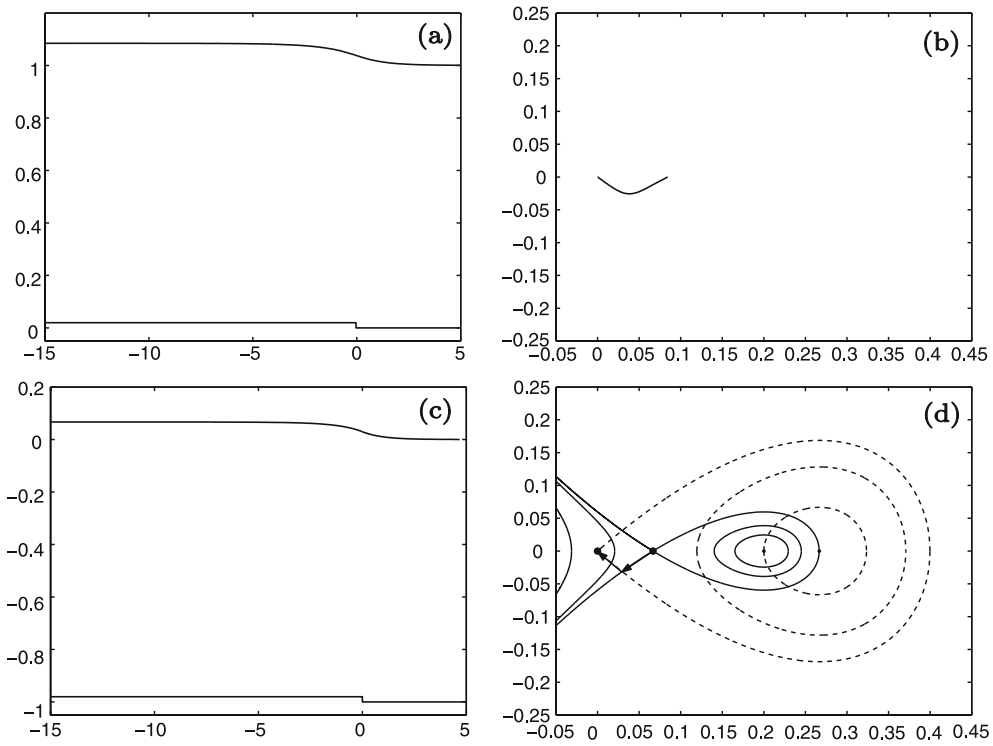

Fig. 4 Supercritical flow for given values of $F = 1.20$ and $h = 0.02$. **a** Nonlinear free-surface profile. The constant elevation as $x \to -\infty$ is $\eta(-\infty) = 0.08$ or $d = 1.08$, which is in full agreement with the analytical value given by Eq. (7) ($d = 1.08$ or $d = 1.22$). The value of the downstream Froude number is $F^* = 1.08$, which is in good agreement with the analytical value given by Eq. (8) ($F^* = 1.09$). **b** Values of $\mathrm{d}y/\mathrm{d}x = \tan\theta$ versus $y - 1 = \eta$, showing the nonlinear phase trajectory for **a**. **c** Weakly nonlinear free-surface profile. The constant elevation as $x \to -\infty$ is $\eta(-\infty) = 0.07$. **d** Weakly nonlinear phase portrait for **c**, $\mathrm{d}\eta/\mathrm{d}x$ versus η. The *solid*, resp. *dashed*, curves correspond to orbits for $x < 0$, resp. $x > 0$. Along the *bold* curve, one has first $C_\mathrm{s} = 0.004$ [see Eq. (19)] and then $C = 0$ [see Eq. (16)]. Among the four fixed points, there are two centre points ($\eta = 0.20, 0.27$) and two saddle points ($\eta = 0, 0.07$)

3.1 Supercritical flow

In this subsection, the step height h is assumed to be positive. Supercritical flows can also be computed for $h < 0$ but they will be discussed in Sect. 3.3. A two-parameter family of supercritical solutions was obtained for given values of $h > 0$ and $F > 1$. In the discretized system coming from the fully nonlinear theory there are N unknowns: θ_I, $I = 1, \ldots, N$. The $N - 1$ equations obtained from [A] combined with the condition that forces the free surface to be flat as $x \to -\infty$ yield N nonlinear algebraic equations in terms of the N unknowns. For given values of $F > 1$ and $h > 0$ (or ϕ_b) this system of equations is solved using an iterative method of Newton's type.

Fig. 4a provides a computed nonlinear free-surface profile with $h = 0.02$ and $F = 1.20$. The constant downstream free-surface elevation $\eta(-\infty) = 0.08$ and the downstream Froude number $F^* = 1.08$ came as part of the solution. Fig. 4b shows a plot of the nonlinear trajectory in the phase plane $\mathrm{d}y/\mathrm{d}x = \tan\theta$ versus $y - 1 = \eta$, for the solution shown in Fig. 4a.

Fig. 4c shows an analytically derived weakly nonlinear free-surface profile for the same given values $h = 0.02$ and $F = 1.20$. The constant free-surface elevation $\eta(-\infty) = 0.07$ far downstream and the downstream Froude number $F^* = 1.12$ came as part of the solution. The agreement between the weakly nonlinear profile in Fig. 4c and the fully nonlinear profile in Fig. 4a is good for these particular values of the Froude number, $F = 1.20$, and step height, $h = 0.02$. With $h = 0.02$, the minimum Froude number corresponding to the right turning point in Fig. 2e is $F = 1.175$. Solutions were computed down to that value. Recall that F^* is then equal to one.

Fig. 4d provides the phase portrait (η, η_x) for the weakly nonlinear solution of Fig. 4c. The dashed curves in Fig. 4d correspond to the flow upstream of the step, $x > 0$, $h = 0$, while the solid curves correspond to the

flow downstream of the step, $x < 0, h > 0$. The bold curve is the weakly nonlinear solution, that connects the two phase portraits (η, η_x).

The number of independent parameters was determined by performing the following analysis in the weakly nonlinear phase plane (η, η_x). For the given value $F = 1.20$, one can plot the dashed phase portrait of Fig. 4d. Fixing $h = 0.02$ then enables us to plot the solid phase portrait of Fig. 4d. The trajectory of the supercritical flow in the phase plane goes from the saddle point $\eta = 0.07$, $\eta_x = 0$ to the saddle point $\eta = 0$, $\eta_x = 0$, via the intersection of the dashed and solid phase portraits. Figure 4b provides a check that our analysis in the weakly nonlinear phase plane (η, η_x) is correct for Fig. 4d.

We obtained qualitatively similar results to those shown in Fig. 4 for the same value of $F = 1.20$ and different values of $0 < h < h_{\max}$. The maximum step height $h_{\max}$ can be quantified both with the fully nonlinear theory and with the weakly nonlinear theory (see Fig. 3e). Recall that in the fully nonlinear case, Eq. (13) shows that

$$h_{\max} = \frac{1}{2}\left(2 + F^2 - 3F^{2/3}\right). \tag{44}$$

In the weakly nonlinear case, considering the limit $\eta_1 \to \eta_2$ in (20) yields

$$h_{\max} = \frac{2}{3}(F-1)^2. \tag{45}$$

With $F = 1.2$, Eq. (44) gives $h_{\max} = 0.0261$ while Eq. (45) gives $h_{\max} = 0.0267$.

Similar supercritical flows with $h > 0$ were computed by King and Bloor [8] (see their Fig. 2). In the next subsection we consider subcritical flows ($F < 1$). Solutions are computed for positive steps as well as negative steps (King and Bloor restricted their study to positive steps).

3.2 Subcritical flow

For subcritical flows, a two-parameter family of solutions was obtained for given values of h and $F < 1$. In the discretized system obtained from the fully nonlinear theory there are N unknowns: θ_I, $I = 1, \ldots, N$. The $N - 1$ equations obtained from [A] and the condition that forces the free surface to be flat as $x \to \infty$ yield N nonlinear algebraic equations in terms of the N unknowns. For given values of $F < 1$ and h, this system of equations is solved as in Sect. 3.1 using an iterative method of Newton's type. We obtained solutions for both $h < 0$ and $h > 0$, see Fig. 5 and 6.

We shall first discuss the solution type for $F < 1$ and $h < 0$. Figure 5a shows a computed nonlinear free-surface profile with $h = -0.01$ and $F = 0.90$. The amplitude of the waves on the downstream free surface, which came as part of the solution, is $A = 0.06$. The corresponding nonlinear phase trajectory is shown in Fig. 5b. Figure 5c provides an analytically derived weakly nonlinear free-surface profile with $h = -0.01$ and $F = 0.90$. The amplitude of the waves on the downstream free surface is $A = 0.07$. The weakly nonlinear and fully nonlinear profiles of Fig. 5a, c are essentially the same for these particular values of the Froude number, $F = 0.90$, and step height, $h = -0.01$. We found that for values of the Froude number $F < 0.90$, the quantitative comparison was not as good. We also found the agreement to be good when $|h|$ was of the order $(F-1)^2$, for given values of $F > 0.90$. This is due to the scalings in the weakly nonlinear theory.

The weakly nonlinear phase plane (η, η_x) is given in Fig. 5d. The dashed curves correspond to the flow upstream of the step, $x > 0$, $h = 0$, and the solid curves correspond to the flow downstream of the step, $x < 0, h < 0$. The solution trajectory in the phase plane is the bold periodic orbit intersecting the centre point $(\eta = 0, \eta_x = 0)$. We determined the number of independent parameters by performing the following analysis in the weakly nonlinear phase plane (η, η_x). For a given value $F = 0.90$, the dashed phase portrait in Fig. 5d can be plotted. Fixing $h = -0.01$ then enables us to plot the solid phase portrait in Fig. 5d. The trajectory of the solution in the phase plane connects the centre point $(\eta = 0, \eta_x = 0)$ (dashed phase portrait) with the inner periodic orbit of the solid phase portrait.

We now consider subcritical flows with $h > 0$. Figure 6a, c show fully nonlinear and weakly nonlinear profiles with $h = 0.01$ and $F = 0.85$.

The agreement between the weakly and nonlinear profiles in Fig. 6a, c is good for the given values of the Froude number, $F = 0.85$, and step height, $h = 0.01$. We found that for values of the Froude number F closer to 1 and when h is of the order $(F-1)^2$, weakly nonlinear and fully nonlinear profiles are in very good agreement. The analysis in the weakly nonlinear phase plane of Fig. 6d is similar to the analysis for

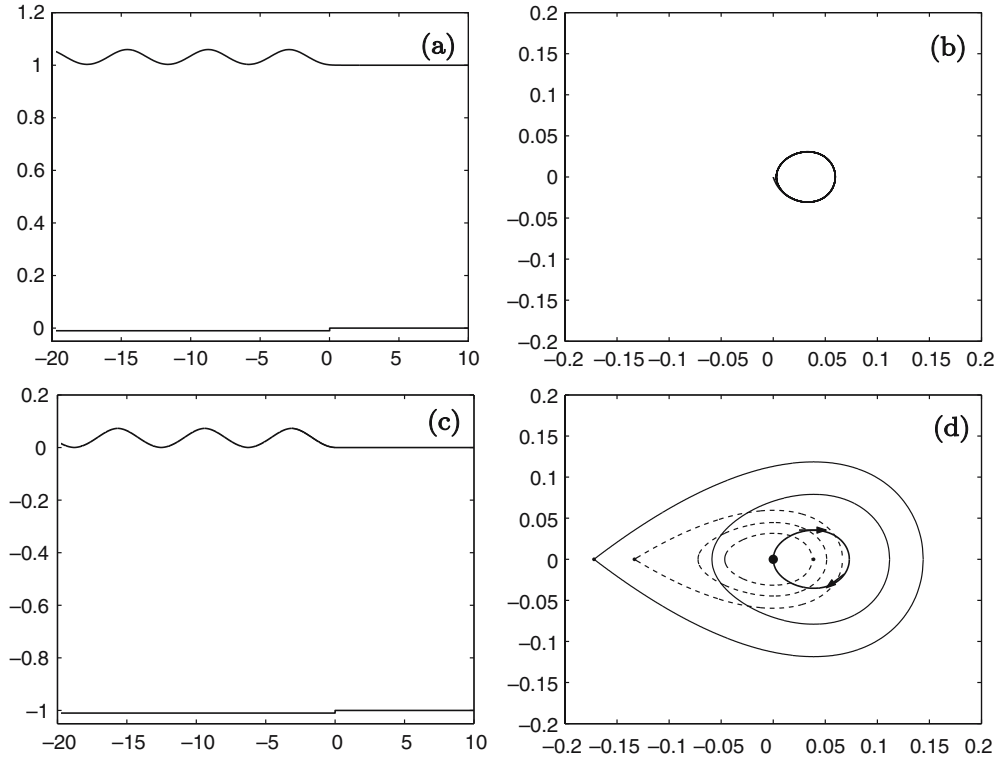

Fig. 5 Subcritical flow with $F = 0.90$ and $h = -0.01$. **a** Nonlinear free-surface profile. The amplitude of the waves is $A = 0.06$. The mean elevation as $x \to -\infty$ is $\eta(-\infty) = 0.03$ or $d = 1.03$, which is in full agreement with the analytical value given by Eq. (7) ($d = 1.03$ or $d = 0.83$), although it was assumed that the flow is uniform as $x \to -\infty$. **b** Phase plane $\mathrm{d}y/\mathrm{d}x = \tan\theta$ versus $y - 1 = \eta$ for **a**. **c** Weakly nonlinear free-surface profile. The amplitude of the waves is $A = 0.07$. **d** Phase plane $d\eta/dx$ versus η for **c**. The *solid*, resp. *dashed*, curves correspond to orbits for $x < 0$, resp. $x > 0$. Along the *bold* curve, one has $C_s = 0$. Among the four fixed points, there are two centre points ($\eta = 0, 0.04$) and two saddle points ($\eta = -0.13, -0.17$)

the solutions with $h < 0$. However, there is one difference: instead of looking for the intersection between a periodic orbit and the origin, one can look for the intersection between the solid homoclinic orbit and the origin. This will be done in Sect. 3.4. The resulting solution is a hydraulic fall, which is in fact a limiting configuration. Indeed, for a given value $F < 1$, as h increases, the fixed points for the region $x < 0$ move closer together and at some point, say $h = h_{\mathrm{front}}$, the tip of the homoclinic orbit will be the origin. Beyond, no bounded solid orbit will be able to reach the origin.

We have presented subcritical flows with negative and positive values of $h < h_{\mathrm{front}}$. Note that for a given Froude number $F < 1$, one can go continuously from a step down to a step up. When $h = 0$, the flow is simply uniform (see Fig. 3a).

Outside the range of validity of the weakly nonlinear theory we computed two nonlinear solutions for a value of the Froude number $F = 0.50$. Figure 7a is for a step height $h = 0.14$ and Fig. 7b is for a step height $h = -0.44$. Note that the numerical scheme can handle steps that are not vertical. Similar solutions were computed by King and Bloor [8], but only for a vertical step with $h > 0$ (see their Fig. 4).

In the next subsection we discuss generalised supercritical flows with $F > 1$ and $h < 0$. Such solutions were first computed by Dias and Vanden-Broeck [4] in the context of channel flows over an obstacle. The flow is supercritical on one side of the step and wavy on the other side.

3.3 Generalised supercritical flow

For generalised supercritical flows, we obtained a one-parameter family of solutions for given values of $h < 0$ and $F > 1$. The parameter can be chosen as the elevation of the free surface at the origin $\eta(0)$. It is shown below how this extra parameter appears naturally in the phase plane.

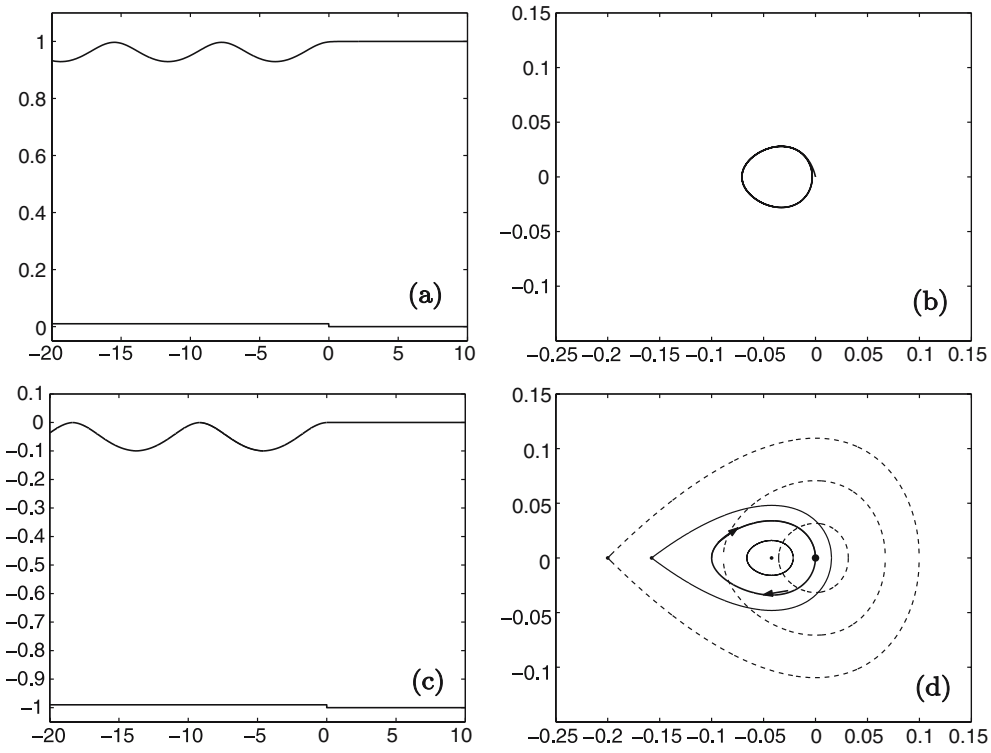

Fig. 6 Subcritical flow with $F = 0.85$ and $h = 0.01$. **a** Nonlinear free-surface profile. The amplitude of the waves is $A = 0.07$. The mean elevation as $x \to -\infty$ is $\eta(-\infty) = -0.03$ or $d = 0.97$, which is in full agreement with the analytical value given by Eq. (7) ($d = 0.97$ or $d = 0.85$), although it was assumed that the flow is uniform as $x \to -\infty$. **b** Phase plane $\mathrm{d}y/\mathrm{d}x = \tan\theta$ versus $y - 1 = \eta$ for **a**. **c** Weakly nonlinear free-surface profile. The amplitude of the waves is $A = 0.10$. **d** Phase plane $\mathrm{d}\eta/\mathrm{d}x$ versus η for **c**. The *solid*, resp. *dashed*, curves correspond to orbits for $x < 0$, resp. $x > 0$. Along the *bold* curve, one has $C_\mathrm{s} = 0$. Among the four fixed points, there are two centre points ($\eta = 0, -0.04$) and two saddle points ($\eta = -0.20, -0.16$)

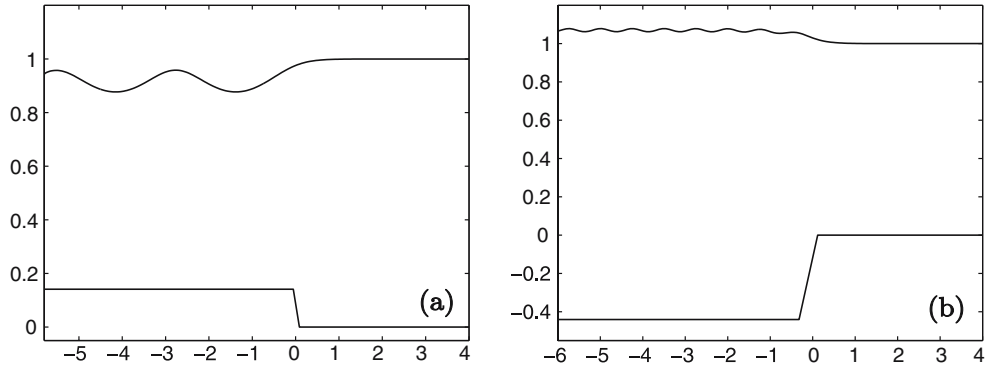

Fig. 7 Nonlinear free-surface profile corresponding to a subcritical flow with $F = 0.50$ and a 45°rise/fall in the step in the bottom of the channel: **a** $h = 0.14$, **b** $h = -0.44$

Figures 8, 9, 10, 11 and 12 show various computed solutions with the same Froude number $F = 1.10$ and step height $h = -0.01$, but different elevations at the origin: $\eta(0) = -0.01, 0, 0.01, 0.02$. The amplitude of the waves on the downstream free surface comes as part of the solution. The mean elevation as $x \to -\infty$ is $\eta(-\infty) = 0.17$ or $d = 1.17$, which is in agreement with the analytical value given by Eq. (7) ($d = 1.17$ or $d = 0.95$), although it was assumed that the flow is uniform as $x \to -\infty$. In the weakly nonlinear approximation, the four fixed points split into two centre points ($\eta = 0.13, 0.17$) and two saddle points ($\eta = 0, -0.04$).

The weakly nonlinear and fully nonlinear profiles in Figs. 8a, 9a, 10a, 11a and 12a and 8c, 9c, 10c, 11c and 12c are in good agreement for these values of the Froude number, $F = 1.10$, and step height, $h = -0.01$. We found that for values of the Froude number $F > 1.15$, the weakly nonlinear and fully nonlinear profiles did

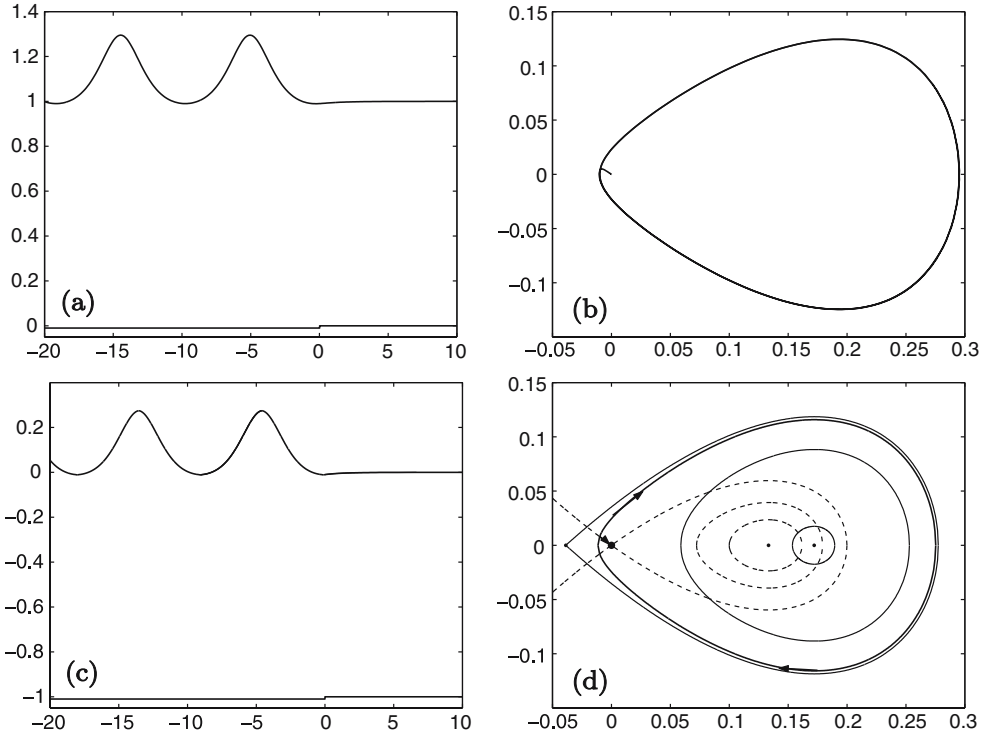

Fig. 8 Generalised supercritical flow with $F = 1.10$, $h = -0.01$ and $\eta(0) = -0.01$. **a** Nonlinear free-surface profile. The amplitude of the waves is $A = 0.31$. **b** Values of $\mathrm{d}y/\mathrm{d}x = \tan\theta$ versus $y - 1 = \eta$ for **a**. **c** Weakly nonlinear free-surface profile. The amplitude of the waves is $A = 0.29$. **d** Phase plane $\mathrm{d}\eta/\mathrm{d}x$ versus η for **c**. Along the bold curve, one has first $C_s = 0.0006$ [see Eq. (19)] and then $C = 0$ [see Eq. (16)]

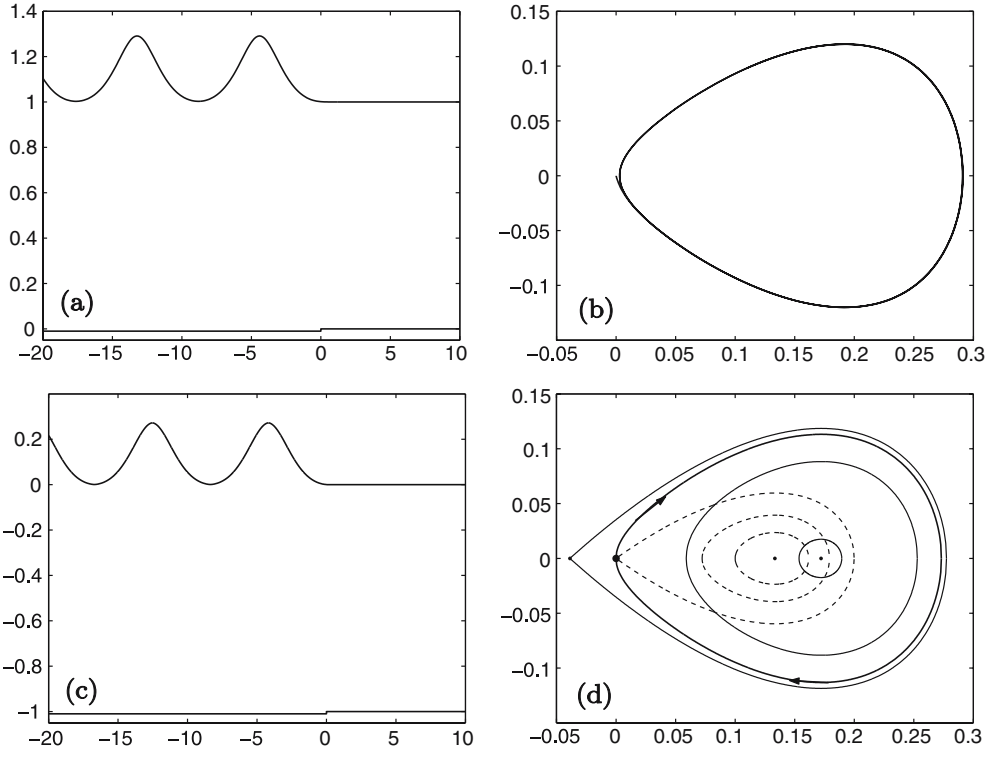

Fig. 9 Same as Fig. 8 with $\eta(0) = 0.00$. The amplitude of the waves is $A = 0.29$ (fully nonlinear) and $A = 0.27$ (weakly nonlinear)

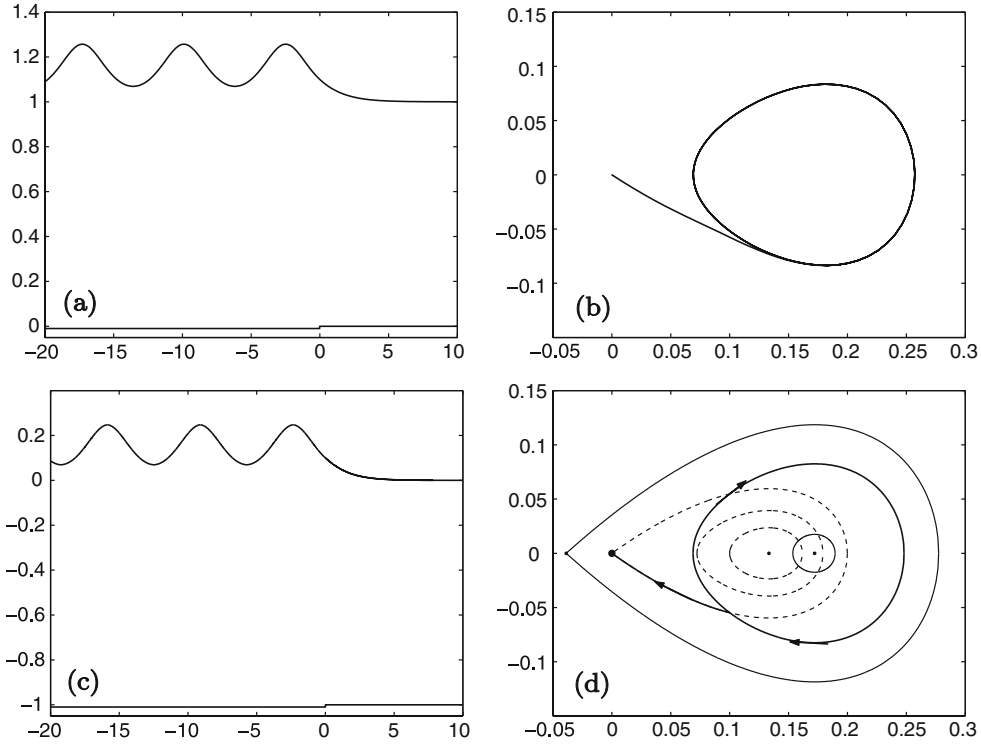

Fig. 10 Same as Fig. 8 with $\eta(0) = 0.10$. The amplitude of the waves is $A = 0.19$ (fully nonlinear) and $A = 0.18$ (weakly nonlinear). Along the *bold* curve, the value of C in Eq. (16) is 0 and the value of C_s in Eq. (19) is -0.006

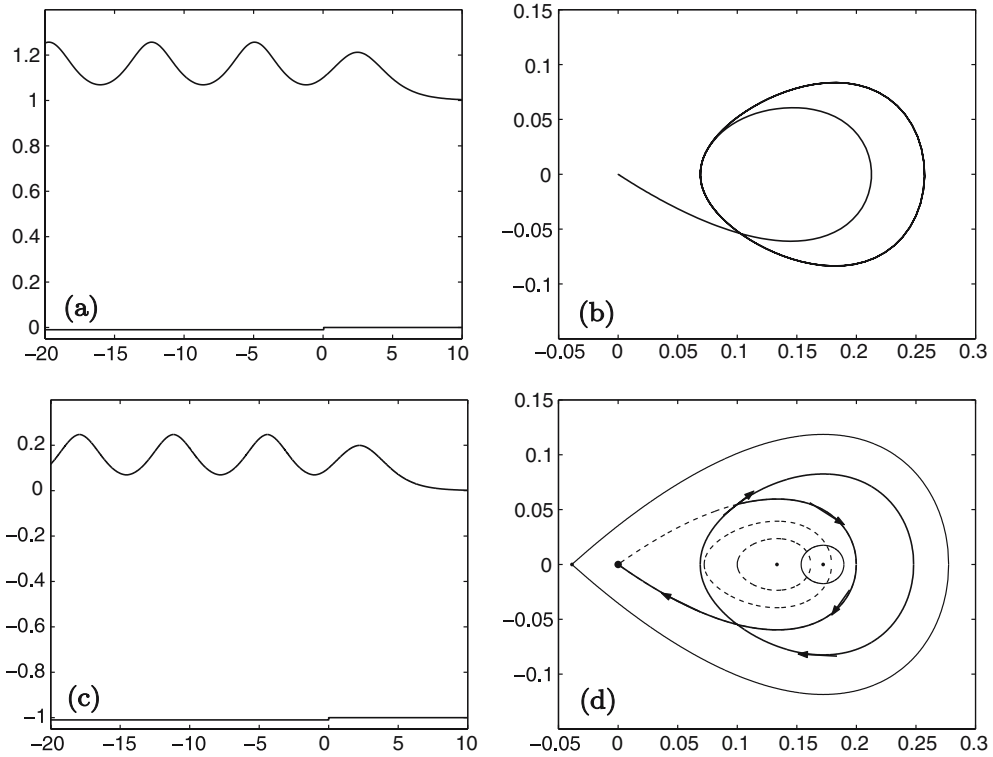

Fig. 11 Same as Fig. 10. The only difference is in the way the transition to the dashed orbit is made

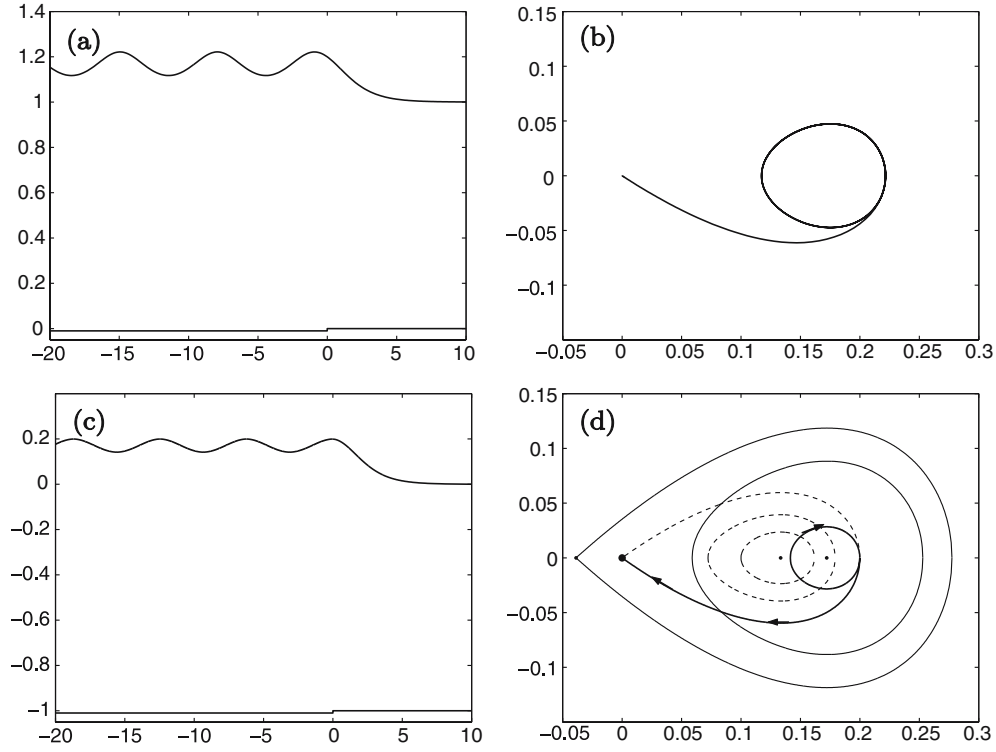

Fig. 12 Same as Fig. 8 with $\eta(0) = 0.20$. The amplitude of the waves is $A = 0.10$ (fully nonlinear) and $A = 0.06$ (weakly nonlinear). The value of C in Eq. (16) is 0 and $C_s = -0.012$ in Eq. (19)

not compare as well quantitatively. We also found that weakly nonlinear and fully nonlinear profiles compared well quantitatively, when $|h|$ was of the order $(F-1)^2$, for given values of F close to 1.

The number of independent parameters was determined by performing the following analysis in the weakly nonlinear phase plane (η, η_x). For the given value $F = 1.10$, the dashed phase portrait in Figs. 8d, 9d, 10d, 11d and 12d can be plotted. Fixing $h = -0.01$ then enables us to plot the solid phase portrait. The trajectory in the phase plane connects the saddle point $(\eta = 0, \eta_x = 0)$ (dashed phase portrait) to an inner periodic orbit of the solid phase portrait. By fixing an extra parameter, one can vary the amplitude A of the waves appearing on the downstream free surface, for the same values of $F = 1.10$ and $h = -0.01$. We chose the extra parameter to be the free-surface elevation at $x = 0$. In terms of the weakly nonlinear theory this extra parameter is related to C_s, see Eq. (19). Changing the parameter C_s determines which inner periodic orbit the solution follows in Fig. 8d, 9d, 10d, 11d and 12d.

In Fig. 12 with $\eta(0) = 0.20$, the fully nonlinear and weakly nonlinear amplitudes of the waves, $A = 0.10$ and $A = 0.06$, and the free-surface profiles do not compare as well as before, at least quantitatively.

In terms of the weakly nonlinear theory for the given values $F = 1.10$ and $h = -0.01$, the profiles shown in Fig. 8c, 9c, 10c, 11c and 12c have a decreasing wave amplitude (from $A = 0.29$ in Fig. 8c to $A = 0.06$ in Fig. 12c).

We note that there are no generalised supercritical flows ($F > 1$) for $h > 0$. This is illustrated in the weakly nonlinear phase plane (η, η_x) of Fig. 4d: it is impossible for the solitary wave solution (dashed curve, $C = 0$) to intersect an inner periodic orbit (solid curves).

At the beginning of Sect. 3.1, we announced that supercritical flows with $h < 0$ would be discussed in the present subsection. Indeed, it is clear from the weakly nonlinear phase planes shown in Fig. 8d, 9d, 10d, 11d and 12d that trajectories leaving from the saddle point on the left, then following the solid homoclinic orbit and finally bifurcating onto the dashed unbounded orbit towards the second saddle point are possible. They correspond to waveless supercritical flows ($F^* > F > 1$) and are qualitatively similar to the bold curve shown in Fig. 4d.

In the next subsection we consider another type of waveless flow with $F > 1$ and $h < 0$ but $F^* < 1$. Such flows are called hydraulic falls.

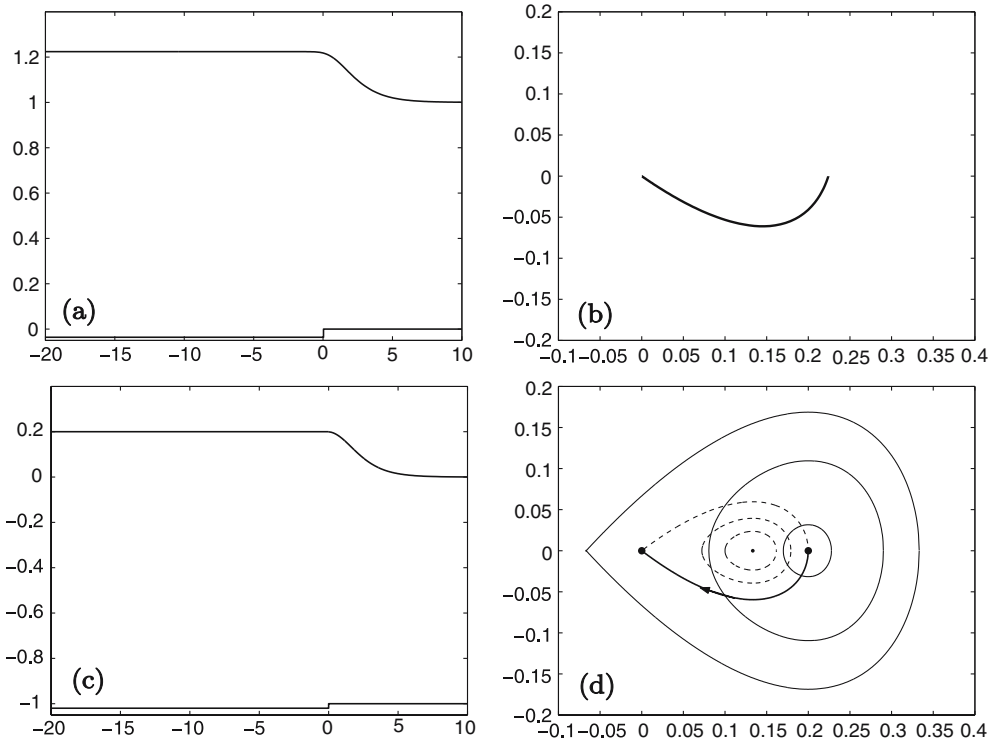

Fig. 13 Hydraulic fall with $F = 1.10$. **a** Nonlinear free-surface profile, with the following computed values: $h = -0.03$, $\eta(-\infty) = 0.22$ (or $d = 1.22$) and $F^* = 0.78$. The analytical values for d given by Eq. (7) are $d = 1.21$ and $d = 0.89$. **b** Trajectory in the phase plane $\mathrm{d}y/\mathrm{d}x = \tan\theta$ versus $y - 1 = \eta$. **c** Weakly nonlinear free-surface profile with $h = -2(F-1)^2 = -0.02$ and $\eta(-\infty) = 2(F-1) = 0.20$. **d** Phase portrait $\mathrm{d}\eta/\mathrm{d}x$ versus η for **c**. Along the *bold* curve, one has $C = 0$ and $C_\mathrm{s} = -0.024$. Among the four fixed points, there are two centre points ($\eta = 0.13, 0.20$) and two saddle points ($\eta = 0, -0.07$)

3.4 Hydraulic falls

Hydraulic falls are solutions that are subcritical on one side of the step and supercritical on the other side. Moreover, the flow is uniform both upstream and downstream. Solutions with $F < 1$, $F^* > 1$ and $h > 0$ or with $F > 1$, $F^* < 1$ and $h < 0$ were found. In each case, it is a one-parameter family of solutions. In other words, the Froude number and the step height cannot be chosen independently.

In terms of the fully nonlinear theory, Eq. (7) has to be satisfied and the free surface is imposed to be flat as $x \to -\infty$. This gives two extra equations:

$$F^2[1 - (y(-\infty) - h)^2] = 2(1 - y(-\infty))(y(-\infty) - h)^2 \tag{46}$$

and

$$\theta_1 = 0. \tag{47}$$

Next we describe how we obtained hydraulic falls. The description is performed for $F > 1$, but the same applies to the case $F < 1$.

For a given value $F > 1$, there are N unknowns, θ_I, $I = 2, \ldots, N$ and h (or ϕ_b). The $N - 1$ equations obtained from [A] and Eq. (46) yield N nonlinear algebraic equations in terms of the N unknowns. For a given Froude number F, this system of equations is solved by using Newton's method.

Figure 13a shows a computed fully nonlinear solution with $F = 1.10$. The downstream constant free-surface elevation $\eta(-\infty) = 0.22$, the downstream Froude number $F^* = 0.78$ and the step height $h = -0.03$ came as part of the solution.

We analytically derived a weakly nonlinear profile for the same Froude number $F = 1.10$, which is shown in Fig. 13c. The values $\eta(-\infty) = 0.20$ and $h = -0.02$ came as part of the solution.

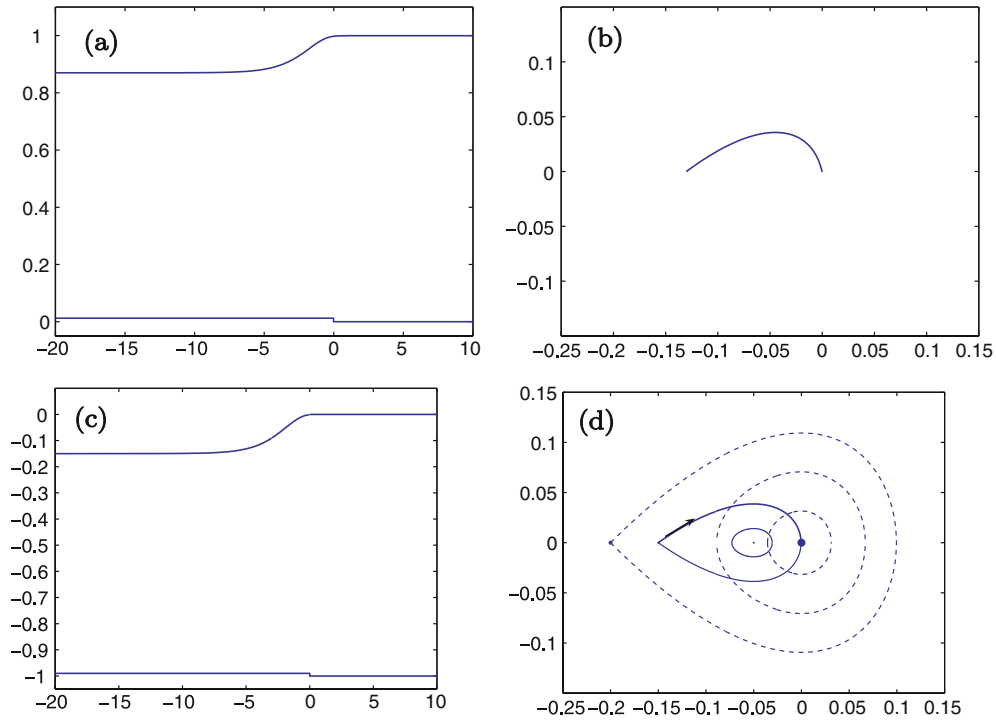

Fig. 14 Hydraulic fall with $F = 0.85$. **a** Nonlinear free-surface profile. The computed elevation of the free surface as $x \to -\infty$ is $\eta(-\infty) = -0.13$ (or $d = 0.87$) and $h = 0.012$. **b** Values of $\mathrm{d}y/\mathrm{d}x = \tan\theta$ versus $y - 1 = \eta$, showing the nonlinear phase trajectory for **a**. **c** Weakly nonlinear free-surface profile. The elevation of the free surface as $x \to -\infty$ is $\eta(-\infty) = F - 1 = -0.15$ and $h = (F-1)^2/2 = 0.011$. **d** Weakly nonlinear phase portrait $\mathrm{d}\eta/\mathrm{d}x$ versus η for **a**. Along the *bold* curve, one has $C = 0$ and $C_\mathrm{s} = 0$. Among the four fixed points, there are two centre points ($\eta = 0, -0.05$) and two saddle points ($\eta = -0.20, -0.15$)

The analysis in the weakly nonlinear phase plane (η, η_x) is shown in Fig. 13d. The dashed curves in Fig. 13d correspond to the flow upstream of the step ($x > 0, h = 0$). The solid curves in Fig. 13d correspond to the flow downstream of the step ($x < 0, h < 0$).

The determination of the number of independent parameters can be understood as follows. For the given value $F = 1.10$, the dashed phase portrait in Fig. 13d can be plotted. The only values that η and η_x can take to ensure that there is an intersection with the centre of the solid phase portrait correspond to the maximum elevation of the dashed solitary wave solution, $\eta = 2(F-1)$ and $\eta_x = 0$. It is easy to show that the height of the step must then be equal to $-2(F-1)^2$. The four fixed points are $\eta = -(2/3)(F-1), 0, (4/3)(F-1), 2(F-1)$. The trajectory in the phase plane then goes from the centre point $\eta = 2(F-1)$ (solid phase portrait) to the saddle point $\eta = 0$, along the solitary wave solution (dashed phase portrait). The constant C in (16) is equal to 0 and the constant C_s in (19) is equal to $-24(F-1)^3$.

Hydraulic falls can also be obtained with $F < 1$. An example is shown in Fig. 14. In the weakly nonlinear approximation, the height of the step must be equal to $(1/2)(F-1)^2$. The four fixed points are $\eta = (4/3)(F-1), F-1, (1/3)(F-1), 0$. The trajectory in the phase plane then goes from the saddle point $\eta = F - 1$ (solid phase portrait) to the centre point $\eta = 0$ (dashed phase portrait), along the solitary wave solution (solid phase portrait). The constants C in (16) and C_s in (19) are equal to 0.

3.5 Flow with $F = 1$

When $h < 0$, the subcritical flows described in subsection Sect. 3.2 can be taken to the limit $F = 1$. Such a solution is shown in Fig. 15 with a step height $h = -0.01$. This solution is a continuous prolongation of the solution shown in Fig. 5. The only difference is in the weakly nonlinear phase plane. The two fixed points for the region $x > 0$ have coalesced into a single fixed point at the origin. The analytical values for d given by Eq. (7) are $d = 1.08, 0.91$. For free-surface flows over an obstacle of compact support, transcritical flows with $F = 1$ are resonant in the longwave limit as energy cannot escape from the forcing. The flow which is observed

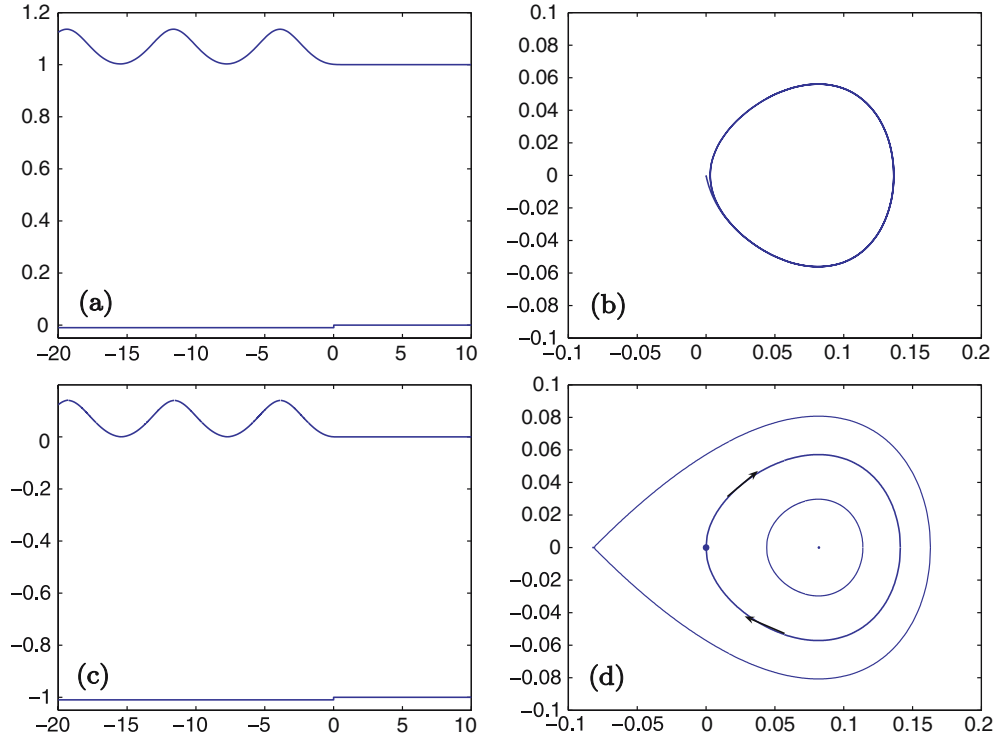

Fig. 15 Flow with $F = 1.00$ and $h = -0.01$. **a** Nonlinear free-surface profile. **b** Values of $\mathrm{d}y/\mathrm{d}x = \tan\theta$ versus $y - 1 = \eta$, showing the nonlinear phase trajectory for **a**. **c** Weakly nonlinear free-surface profile. **d** Weakly nonlinear phase portrait $\mathrm{d}\eta/\mathrm{d}x$ versus η for **a**. Along the *bold* curve, $C_s = 0$. The fixed points are the double point $\eta = 0$, the centre point $\eta = 0.08$ and the saddle point $\eta = -0.08$

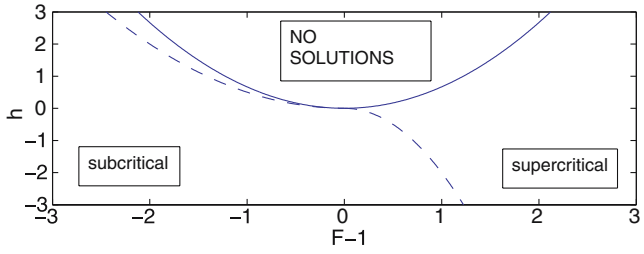

Fig. 16 Solutions for the flow past a step in the plane $(h, F - 1)$. The *dashed lines* correspond to the approximate results given by the weakly nonlinear theory for hydraulic falls. The *solid line* corresponds to the approximate result given by the weakly nonlinear theory for the maximum step height. For subcritical flows, there are no solutions between the dashed and the solid line

physically is then nonsteady for all time. Whether or not the same energy/group velocity argument leading to resonance applies for a step forcing is an open question. However, Zhang and Zhu [16], who integrated numerically the time-dependent forced KdV equation for the flow over a step, found steady transcritical flows for a step down (negative forcing).

4 Conclusions

Free-surface flows past a semi-infinite step in the bottom of a channel have been investigated. Performing an analysis in the weakly nonlinear phase plane (η, η_x) enabled us to systematically identify all the possible types of solutions and the number of independent parameters. The solution trajectory in the phase plane (η, η_x) is the intersection of two orbits originating from two different phase portraits, one upstream of the step and one downstream of the step. Solutions that do not satisfy the radiation condition can be made physical by

introducing another disturbance (for example a pressure distribution on the free surface) into the channel in order to eliminate the waves or by considering a step of finite length. This is ongoing research.

A summary of the solutions considered in this paper is shown in Fig. 16. Many new qualitatively different types of solutions have been presented in this paper. Whether or not these solutions are physically observable is a question of interest, which has not been addressed in this paper. Studies in the spirit of those by Grimshaw and Smyth [7] and Smyth [13] are left for future work. The question of what happens when there is non-existence of steady flows is also of interest.

References

1. Binder, B.J., Vanden-Broeck, J.-M.: Free surface flows past surfboards and sluice gates. Eur. J. Appl. Math. **16**, 601–619 (2005)
2. Binder, B.J., Vanden-Broeck, J.-M., Dias, F.: Forced solitary waves and fronts past submerged obstacles. Chaos **15**, 037106-1–13 (2005)
3. Dias, F., Vanden-Broeck, J.-M.: Open channel flows with submerged obstructions. J. Fluid Mech. **206**, 155–170 (1989)
4. Dias, F., Vanden-Broeck, J.-M.: Generalised critical free-surface flows. J. Eng. Math. **42**, 291–301 (2002)
5. Dias, F., Vanden-Broeck, J.-M.: Trapped waves between submerged obstacles. J. Fluid Mech. **509**, 93–102 (2004)
6. Forbes, L.-K.: Critical free-surface flow over a semi-circular obstruction. J. Eng. Math. **22**, 3–13 (1988)
7. Grimshaw, R.H.J., Smyth, N.: Resonant flow of a stratified fluid over topography. J. Fluid Mech. **169**, 429–464 (1986)
8. King, A.C., Bloor, M.I.G.: Free-surface flow over a step. J. Fluid Mech. **182**, 193–208 (1987)
9. King, A.C., Bloor, M.I.G.: Free-surface flow of a stream obstructed by an arbitrary bed topography. Q. J. Mech. Appl. Math. **43**, 87–106 (1990)
10. Lee, S.-J., Yates, G.T., Wu, T.Y.: Experiments and analysis of upstream-advancing solitary waves generated by moving disturbances. J. Fluid Mech. **199**, 569–593 (1989)
11. Shen, S.S.-P.: On the accuracy of the stationary forced Korteweg–de Vries equation as a model equation for flows over a bump. Q. Appl. Math. **53**, 701–719 (1995)
12. Shen, S.S., Gong, L.: Solitary waves on a shelf. Phys. Fluids A **5**, 1071–1073 (1993)
13. Smyth, N.F.: Modulation theory solution for resonant flow over topography. Proc. R. Soc. Lond. A **409**, 79–97 (1987)
14. Vanden-Broeck, J.-M.: Numerical calculations of the free-surface flow under a sluice gate. J. Fluid Mech. **330**, 339–347 (1996)
15. Yasuda, T., Mutsuda, H., Mizutani, N.: Kinematics of overturning solitary waves and their relations to breaker types. Coast. Eng. **29**, 317–346 (1997)
16. Zhang, Y., Zhu, S.: Subcritical, transcritical and supercritical flows over a step. J. Fluid Mech. **333**, 257–271 (1997)